PAPER

A new treatment of nonlocality in scattering process

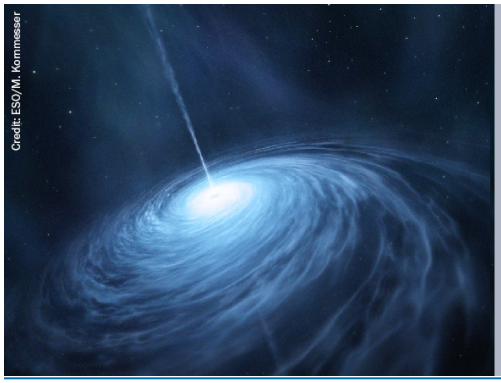

IOP Publishing Journal of Physics G: Nuclear and Particle Physics
J. Phys. G: Nucl. Part. Phys. **45** (2018) 015106 (14pp) https://doi.org/10.1088/1361-6471/aa9877

A new treatment of nonlocality in scattering process

N J Upadhyay[1], **A Bhagwat and B K Jain**

UM-DAE Centre for Excellence in Basic Sciences, Vidyanagari, Mumbai-400098, India

E-mail: neelam.upadhyay@cbs.ac.in, ameeya@cbs.ac.in and brajeshk@gmail.com

Received 24 December 2016, revised 31 October 2017
Accepted for publication 6 November 2017
Published 13 December 2017

Abstract

Nonlocality in the scattering potential leads to an integro-differential equation. In this equation nonlocality enters through an integral over the nonlocal potential kernel. The resulting Schrödinger equation is usually handled by approximating r,r'-dependence of the nonlocal kernel. The present work proposes a novel method to solve the integro-differential equation. The method, using the mean value theorem of integral calculus, converts the nonhomogeneous term to a homogeneous term. The effective local potential in this equation turns out to be energy independent, but has relative angular momentum dependence. This method is accurate and valid for any form of nonlocality. As illustrative examples, the total and differential cross sections for neutron scattering off ^{12}C, ^{56}Fe and ^{100}Mo nuclei are calculated with this method in the low energy region (up to 10 MeV) and are found to be in reasonable accord with the experiments.

Keywords: neutron nucleus scattering, nonlocal kernel, nonlocality

(Some figures may appear in colour only in the online journal)

1. Introduction

The nucleon–nucleus interaction is known to be nonlocal in nature [1–3]. This nonlocal character arises because of the many-body effects such as the virtual excitations in the nucleus and the exchange of the nucleons within the interacting system [2–5]. The explicit use of the nonlocal interaction framework, therefore, enriches the theoretical description of the scattering process. Its incorporation, however, leads to the integro-differential form of the Schrödinger equation, which is difficult to solve. It is written as:

[1] Author to whom any correspondence should be addressed.

$$\left[\frac{\hbar^2}{2\mu}\nabla^2 + E + V_{\rm SO}\mathbf{L}\cdot\boldsymbol{\sigma}\right]\Psi(\mathbf{r}) = \int V(\mathbf{r},\,\mathbf{r}')\Psi(\mathbf{r}')\mathrm{d}\mathbf{r}', \tag{1}$$

where μ is the reduced mass of the nucleon–nucleus system, E is the center of mass energy, $(V_{\rm SO}\,\mathbf{L}\cdot\boldsymbol{\sigma})$ is the local spin-orbit interaction, $V(\mathbf{r},\,\mathbf{r}')$ is the nonlocal interaction kernel and $\Psi(\mathbf{r})$ is the scattering wave function.

Any effort to solve equation (1) requires the explicit form of $V(\mathbf{r},\,\mathbf{r}')$, which, unfortunately, is not known. However, it is expected that this form should be such that in the limit of vanishing nonlocality, the integro-differential equation reduces to the conventional homogeneous equation. Guided by this idea, a factorized form for the nonlocal kernel was proposed by Frahn and Lemmer [2, 3], which is written as

$$V(\mathbf{r},\,\mathbf{r}') = \frac{1}{\pi^{3/2}\beta^3}\exp\left[-\frac{|\mathbf{r}-\mathbf{r}'|^2}{\beta^2}\right]U\left(\frac{|\mathbf{r}+\mathbf{r}'|}{2}\right), \tag{2}$$

where β is the range parameter and U is the nonlocal interaction. The term with β represents the behavior of nonlocality. It reduces to the Dirac δ function in the limit of vanishing nonlocality. This prescription has been used by several groups, some of the notable amongst them being the work of Perey and Buck [6] and Tian *et al* [7]. The important aspect of the former study [6] is the construction of the energy dependent local equivalent potential which can be used in the homogeneous Schrödinger equation. This result is obtained by using the gradient approximation, which is found to be reliable for tightly bound nuclei. However, for nuclei away from the stability line its validity might be a suspect. In the other study, Tian *et al* [7] have treated nonlocality by solving equation (1) using Lanczos method [8, 9].

Other approaches to obtain efficient solution to equation (1) with a general nonlocal kernel include writing the nonlocal kernel in separable form [10, 11], expanding nonlocal kernel in terms of Chebyshev polynomials [12], to name a few. Recently a microscopic approach to address nonlocality has been developed by Rotureau *et al* [13] wherein the nonlocal optical potential for nucleon–nucleus scattering is constructed from chiral interactions. These methods, however, might have computational limitations in analyzing the nucleon–nucleus scattering data routinely.

In this article we present a readily implementable technique to solve the integro-differential Schrödinger equation. With a very simple approximation, this technique reduces the integro-differential equation to a homogeneous differential equation. This is achieved by using the mean value theorem (MVT) of integral calculus [14]. Application of the MVT converts the nonlocal interaction to a local form. This local potential is energy independent, but depends upon relative angular momentum (l). The important aspect of this method is that it does not depend upon any particular choice of the nonlocal form factor and computationally it is very tractable.

The paper is organized as follows: in section 2 we present the MVT technique used to reduce the integro-differential equation to a homogeneous one and identify the requirements for its applicability. The accuracy of the solution of the homogeneous equation is established in section 3. As our method is applicable to any choice of the nonlocal form factor, we study its applicability for different choices in section 4. Finally, section 5 is devoted to the comparison of the predictions of our method with the experimental observables like, total and differential cross sections. As illustrations, we have studied neutrons scattering off ^{12}C, ^{56}Fe and ^{100}Mo targets.

2. Method to solve the integro-differential equation

For the present, dropping the spin-orbit term in equation (1) we write partial wave expansion for the scattering wave function, Ψ, and the nonlocal potential, $V(\mathbf{r}, \mathbf{r}')$, as

$$\Psi(\mathbf{r}) = \sum_{l,m_l} i^l \frac{u(l; r)}{r} Y_{lm_l}(\Omega_r) \text{ and} \tag{3}$$

$$V(\mathbf{r}, \mathbf{r}') = \sum_{l',m_l'} \frac{g(l'; r, r')}{rr'} Y_{l'm_l'}(\Omega_r) Y^*_{l'm_l'}(\Omega_{r'}) \tag{4}$$

respectively. The resulting Schrödinger equation for the lth partial wave is

$$\left[\frac{\mathrm{d}^2}{\mathrm{d}r^2} - \frac{l(l+1)}{r^2} + \frac{2\mu E}{\hbar^2}\right] u(l; r) = \frac{2\mu}{\hbar^2} \int_0^{r_m} g(l; r, r') u(l; r') \mathrm{d}r'. \tag{5}$$

The upper limit of the integration over nonlocal kernel, $g(l; r, r')$, is the matching radius (r_m) at which its contribution to the integral becomes negligible. The nonlocal kernel for lth partial wave is written as

$$g(l; r, r') = \left(\frac{2rr'}{\sqrt{\pi}\,\beta^3}\right) \exp\left(\frac{-r^2 - r'^2}{\beta^2}\right) \times \int_{-1}^{1} U\left(\frac{|\mathbf{r} + \mathbf{r}'|}{2}\right) \exp\left(\frac{2rr'\cos\theta}{\beta^2}\right) P_l(\cos\theta) \mathrm{d}(\cos\theta), \tag{6}$$

where θ is the angle between the vectors $\mathbf{r}$ and $\mathbf{r}'$ [6]. In the literature [6], $|\mathbf{r} + \mathbf{r}'|$ is approximated as $(r + r')$ leading to

$$g(l; r, r') = \left(\frac{2rr'}{\sqrt{\pi}\,\beta^3}\right) \exp\left(\frac{-r^2 - r'^2}{\beta^2}\right) U\left(\frac{r + r'}{2}\right) \times \int_{-1}^{1} \exp\left(\frac{2rr'\cos\theta}{\beta^2}\right) P_l(\cos\theta) \mathrm{d}(\cos\theta). \tag{7}$$

However, in the present work we do not use the above approximation. The integral appearing in equation (6) is evaluated numerically. Since equation (7) is used very often in the literature, effect of the approximation leading to it is examined explicitly later in section 3.2.

2.1. The nonlocal potential, U(r)

The construction of the non-local kernel requires the nucleon-nucleus potential, $U(r)$. Since in the present work our aim is to propose a new treatment of nonlocality and establish its correctness, we prefer to have a well-established prescription for $U(r)$ that is applicable to most of the nuclei. The primary choice is the conventional Wood–Saxon form commonly used in the local optical model calculations:

$$U(x) = -(V_r f_r(x) + \mathrm{i}W_i f_i(x) + \mathrm{i}W_d f_d(x)) \tag{8}$$

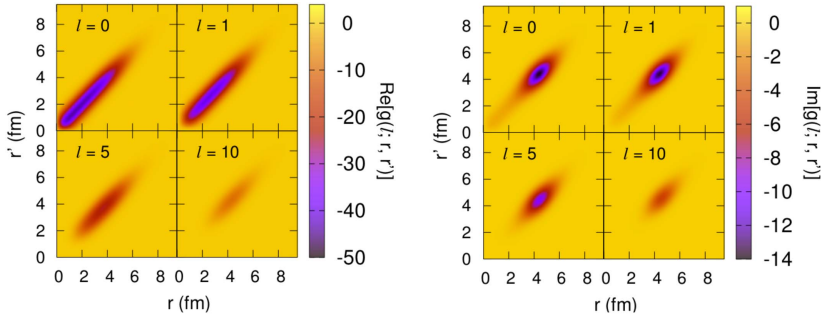

(a) Real part (b) Imaginary Part

Figure 1. Behavior of the nonlocal kernel as a function of relative coordinates r and r' for $l = 0$, 1, 5 and 10. Calculations are done with TPM15 parameterization for neutron scattering off ^{56}Fe nucleus [7]. The non-local range used in calculations is $\beta = 0.90$ fm.

$$\text{with } f_y(x) = \left[1 + \exp\left(\frac{x - R_y}{a_y}\right)\right]^{-1} \quad y = r \text{ and } i$$

$$f_d(x) = 4\exp\left(\frac{x - R_d}{a_d}\right)\left[1 + \exp\left(\frac{x - R_d}{a_d}\right)\right]^{-2}. \tag{9}$$

Recently Tian *et al* [7] have obtained a new set of parameters for this type of potential by fitting the nucleon scattering data on nuclei ranging from ^{27}Al to ^{208}Pb with incident energies around 10–30 MeV. It provides an excellent agreement with large amount of cross section data and is energy independent. The numerical values of these parameters can be found in table 2 of [7]. Henceforth, the potential obtained by this parameterization will be referred to as 'TPM15'.

2.2. The nonlocal kernel

We now examine the behavior of the nonlocal kernel, $g(l; r, r')$, appearing in the non-homogeneous term in equation (5). To illustrate, we plot $g(l; r, r')$ as a function of r and r' for different partial waves in figure 1 for neutron–^{56}Fe scattering. As it can be seen, $g(l; r, r')$ is a well-behaved function which is symmetric around $r = r'$. Its strength diminishes with increasing l and so does the importance of the nonlocality. This behavior of $g(l; r, r')$ prompts us to use the (MVT of integral calculus [14] to solve the integro-differential equation (equation (5)).

2.3. The MVT technique

According to the MVT of integral calculus [14], if a function $q(x)$ is non-negative and integrable on $[a, b]$ and $p(x)$ is continuous on $[a, b]$, then there exists $c \in [a, b]$ such that

$$\int_a^b p(x)q(x)\mathrm{d}x = p(c)\int_a^b q(x)\mathrm{d}x. \tag{10}$$

The theorem holds for non-positive $q(x)$ as well.

We examine the applicability of this theorem to the kernel in equation (5). The integrand in equation (5) is a product of $g(l; r, r')$ and the wave function, $u(l; r')$. The wave function is continuous in the interval $[0, r_m]$. The analytic structure of $g(l; r, r')$ makes it evident that the

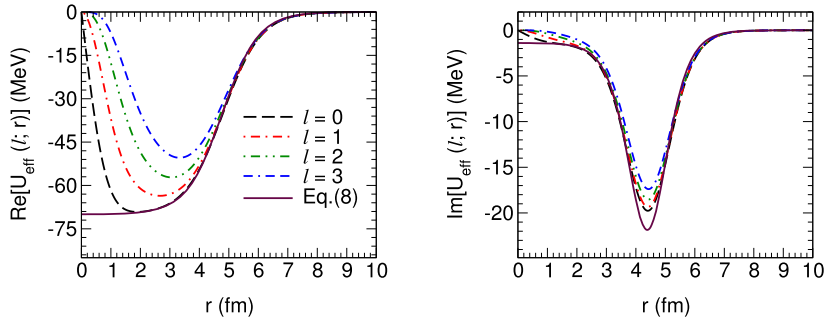

Figure 2. Behavior of $U_{\rm eff}(l;\, r)$ as a function of distance for $l = 0$, 1, 2 and 3. Calculations are done with TPM15 parameterization for n–^{56}Fe scattering [7]. The non-local range used in calculations is $\beta = 0.90$ fm.

kernel is integrable. Considering the behavior of $g(l;\, r,\, r')$ from figure 1, the integral in equation (5) can be written as

$$\int_0^{r_m} g(l;\, r,\, r')u(l;\, r')\mathrm{d}r' = u(l;\, \xi)\int_0^{r_m} g(l;\, r,\, r')\mathrm{d}r' \tag{11}$$

with $\xi \in [0,\, r_m]$. Further, from figure 1 it can be seen that $g(l;\, r,\, r')$ is strongly peaked at $r = r'$ and is symmetric around it. With this observation, we can expand $u(l;\, \xi)$ about $r = r'$. The leading term $u(l;\, r)$, evidently, is the most dominant in the expansion. Therefore, we choose $u(l;\, \xi) = u(l;\, r)$, yielding

$$\int_0^{r_m} g(l;\, r,\, r')u(l;\, r')\mathrm{d}r' \approx u(l;\, r)\int_0^{r_m} g(l;\, r,\, r')\mathrm{d}r'. \tag{12}$$

This leads to the homogenized form of the Schrödinger equation

$$\left[\frac{\mathrm{d}^2}{\mathrm{d}r^2} - \frac{l(l+1)}{r^2} + \frac{2\mu E}{\hbar^2}\right]u(l;\, r) = \frac{2\mu U_{\rm eff}(l;\, r)}{\hbar^2}u(l;\, r), \tag{13}$$

where the effective local potential, $U_{\rm eff}(l;\, r)$, is given by

$$U_{\rm eff}(l;\, r) = \int_0^{r_m} g(l;\, r,\, r')\mathrm{d}r'. \tag{14}$$

This potential contains the most dominant effect of nonlocality. It is independent of energy, but depends on l. In figure 2 we show $U_{\rm eff}(l;\, r)$ in comparison with the TPM15 potential (equation (8)) for neutron–^{56}Fe system. It is observed that $U_{\rm eff}(l;\, r)$ gets reduced in strength as well as modified in shape. This is unlike the local equivalent potential in Perey and Buck's work [6].

3. Accuracy of the method

The homogenized Schrödinger equation (equation (13)) obtained for the description of equation (5), of course, is very neat and useful, but it has an approximation of calculating the kernel at $r = r'$. This needs to be tested carefully. For this purpose we need to compare the solution of the homogeneous equation with that of the original integro-differential equation (equation (5)). This is achieved by solving equation (5) using an iterative scheme. This scheme is initiated by the solution of equation (13) using a suitable boundary condition. The subsequent higher order solutions are obtained with the help of the following iterative

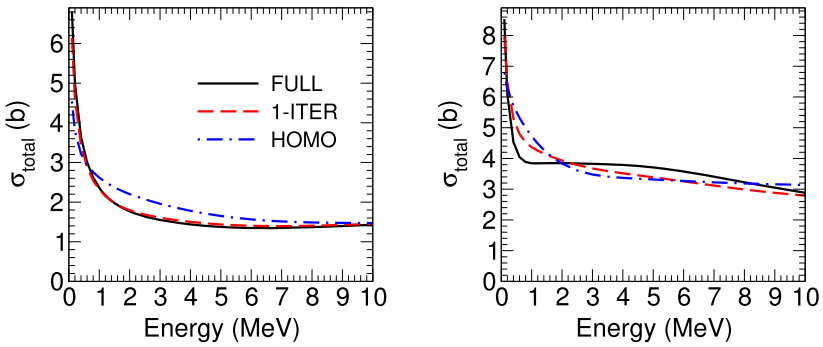

(a) n-^{12}C scattering (b) n-^{56}Fe scattering

Figure 3. Total cross sections for neutron scattering off ^{12}C and ^{56}Fe nuclei. Calculations are done with TPM15 parameterization [7].

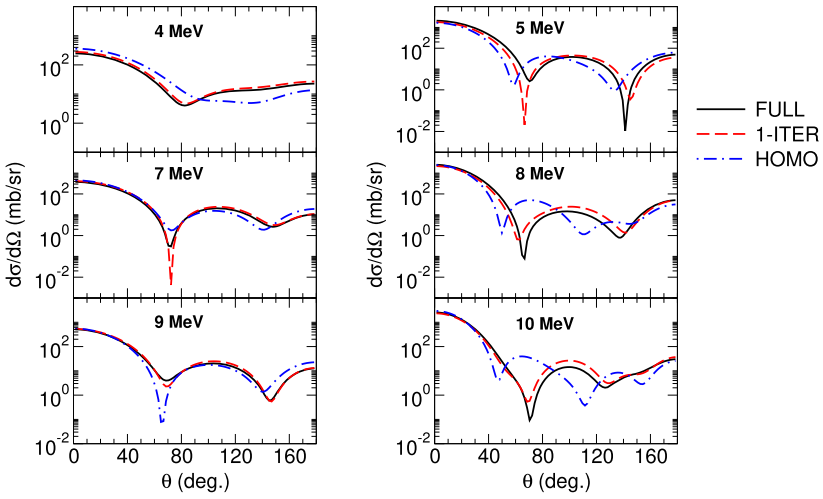

(a) n-^{12}C scattering (b) n-^{56}Fe scattering

Figure 4. Angular distributions for neutron scattering off ^{12}C and ^{56}Fe nuclei. Calculations are done with TPM15 parameterization [7].

scheme:

$$\left[\frac{\mathrm{d}^2}{\mathrm{d}r^2} - \frac{l(l+1)}{r^2} + \frac{2\mu E}{\hbar^2} - \frac{2\mu\, U_{\mathrm{eff}}(l;\, r)}{\hbar^2}\right] u_{i+1}(l;\, r)$$
$$= \frac{2\mu}{\hbar^2}\int_0^{r_m} g(l;\, r,\, r')u_i(l;\, r')\mathrm{d}r' - \frac{2\mu U_{\mathrm{eff}}(l;\, r)}{\hbar^2}u_i(l;\, r), \quad (\text{for all } i \geqslant 0). \tag{15}$$

The iterations are continued till the absolute value of difference between the logarithmic derivatives of the wave function at the matching radius in the ith and the $(i+1)$th steps is less than or equal to 10^{-6}.

In figures 3 and 4 we show the calculated total and differential cross sections for n–^{12}C and n–^{56}Fe scatterings in the low energy domain for various approximations to equation (5).

Results obtained by solving equations (13) and (15) are labeled as HOMO and FULL respectively. To understand the impact of the iterative scheme, in figures 3 and 4 we also show results obtained after one iteration (labeled as 1-ITER). We notice that though the homogeneous results have significant difference (especially for ^{56}Fe) from the FULL results, they are, overall, not far away from them. The 1-ITER results, however, are pretty close to the full results of equation (5). This is very nice, because in actual calculations one can then use just one iteration and get results very close to the FULL results. Computationally, once we have homogeneous results it is straight forward to get 1-ITER results.

3.1. Dependence on the choice of U(r)

To examine further the dependence of the accuracy of our method on the choice of $U(r)$, we perform above calculations for another potential. We construct $U(r) = V(r) + \mathrm{i}W(r)$ such that $V(r)$ is obtained microscopically through folding model [15]:

$$V(r) = \int \mathrm{d}\mathbf{r}_2\, \rho(\mathbf{r}_2) v(r_{12}), \tag{16}$$

where $v(r_{12})$ is the effective nucleon–nucleon interaction, $\rho(\mathbf{r}_2)$ is the total nucleon density of the target and r_{12} is the distance between the projectile (neutron) and a nucleon in the target nucleus. To make it a reasonable representation for the present study, TPM15 parameterization (see equations (8) and (9)) is used for $W(r)$. This prescription of $U(r)$ will be referred to as 'FoldTPM15' in subsequent discussions.

For the effective nucleon–nucleon interaction we have used the well known M3Y prescription [16]:

$$v(r) = \left[7999\,\frac{\mathrm{e}^{-4r}}{4r} - 2134\,\frac{\mathrm{e}^{-2.5r}}{2.5r}\right]\mathrm{MeV}, \tag{17}$$

where the two Yukawa terms represent the direct contribution of the interaction. In principal, one needs to take into account the knock-on contribution as well [15]. Since the knock-on contribution in the nucleon–nucleus scattering is expected to be insignificant in the low energy range [4], we have not included it in equation (17). The density distribution of target nucleus has been calculated using the well established relativistic mean field model [17], which is known to reproduce ground state properties of nuclei spanning the entire periodic table.

In figure 5(a), we show the behavior of the real part of the nonlocal kernel function calculated using FoldTPM15 prescription for neutron scattering off ^{56}Fe. It has the required structure of being well behaved and symmetric about $r = r'$ for the applicability of the MVT technique. We also show the corresponding real part of $U_{\mathrm{eff}}(l; r)$ in figure 5(b).

Comparing the contour plot for $g(l; r, r')$ (see figure 5(a)) with the earlier plot in figure 1 for TPM15, we also notice that the effect of nonlocality in it probably is much less.

The calculated total and differential cross sections shown in figures 6 and 7 are for (i) solution of the homogeneous equation, (ii) solution obtained after one iteration and (iii) converged solution of equation (15) for n–^{12}C and n–^{56}Fe scatterings. The conclusion about the accuracy of our technique in this case, if anything, is better than that seen in figures 3 and 4. Thus, we conclude that the accuracy of our technique is good. This

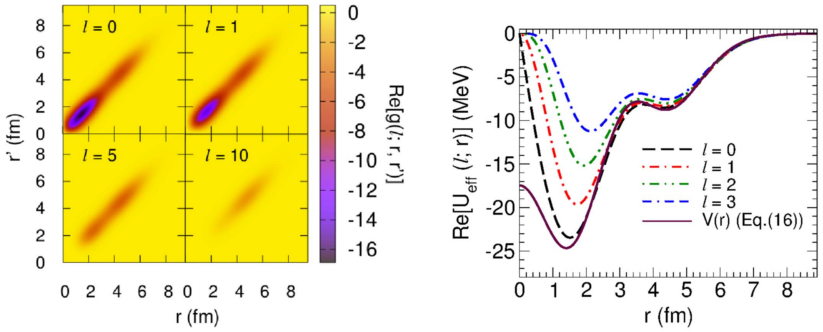

(a) The nonlocal kernel (b) $U_{\rm eff}(l;r)$

Figure 5. Behavior of the real part of the nonlocal kernel and $U_{\rm eff}(l;\,r)$ for neutron scattering off ^{56}Fe nucleus. Calculations are done with FoldTPM15 prescription. The non-local range used in calculations is $\beta = 0.90$ fm.

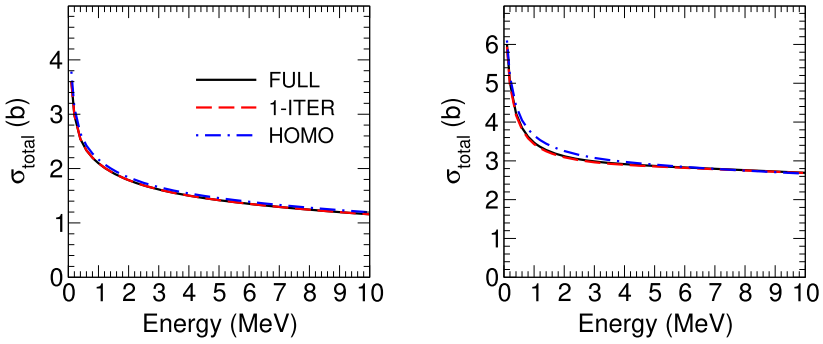

(a) n-^{12}C scattering (b) n-^{56}Fe scattering

Figure 6. Total cross sections for neutron scattering off ^{12}C and ^{56}Fe nuclei. Calculations are done with FoldTPM15 prescription.

improvement in accuracy, as mentioned above, may be due to lesser effect of nonlocality in FoldTPM15.

3.2. Impact of approximation leading to equation (7)

As mentioned in section 2, the nonlocal kernel represented by equation (6) contains the nonlocal potential, $U\left(\frac{|\,\mathbf{r}+\mathbf{r}'\,|}{2}\right)$ inside the integrand. Common practice is to approximate $|\mathbf{r}+\mathbf{r}'|$ by $(r+r')$ leading to equation (7). We study the impact of this approximation on the accuracy of results obtained by solving equation (15). In figure 8, we compare the total cross sections obtained by using equation (6) in (15) with those obtained by using equation (7). Results are shown for neutron scattering off ^{12}C and ^{56}Fe targets using TPM15 parameterization. We find that use of equation (7) in (15) is good within 1% in the considered energy range.

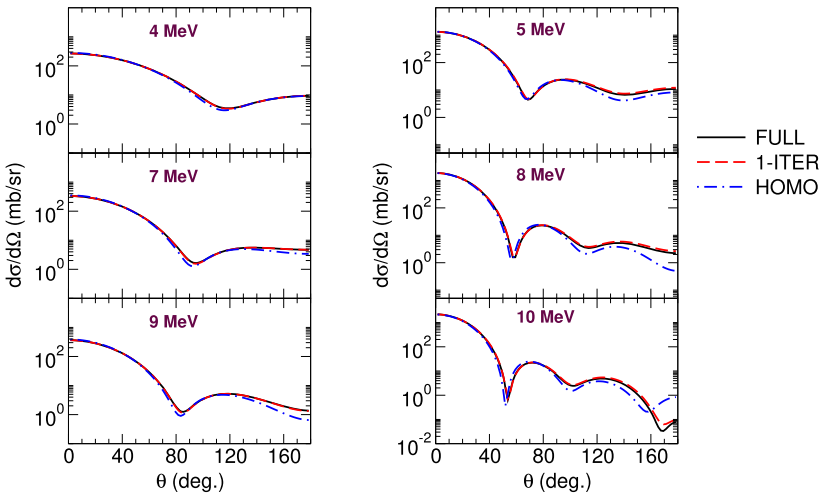

(a) n-^{12}C scattering (b) n-^{56}Fe scattering

Figure 7. Angular distributions for neutron scattering off ^{12}C and ^{56}Fe nuclei. Calculations are done with FoldTPM15 prescription.

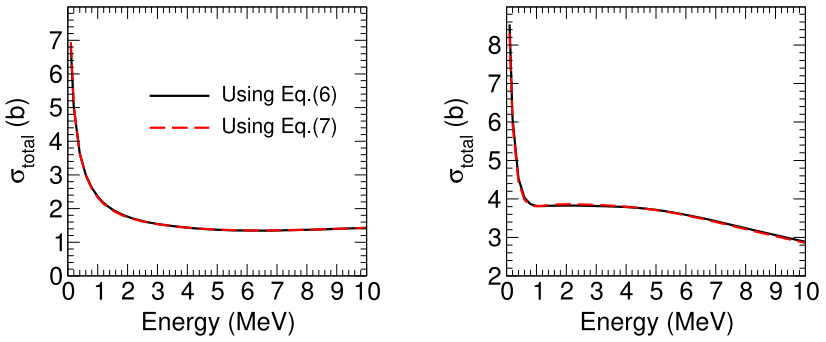

(a) n-^{12}C scattering (b) n-^{56}Fe scattering

Figure 8. Total cross sections calculated using equations (6) and (7) for neutron scattering off ^{12}C and ^{56}Fe nuclei. Calculations are done with TPM15 parameterization [7].

4. Impact of different choice of nonlocal form factor

4.1. Impact of the form of nonlocality

Recently Rotureau *et al* have developed a method to construct nonlocal optical potential from first principle [13]. In such microscopic approach, since the nonlocality is inherent in the formalism, its form could be different from a Gaussian. Therefore, to determine the impact of different choices of nonlocal form factor, we take, in addition to the Gaussian form used so far, an exponential form: $\exp(-|\vec{r} - \vec{r}'|/\alpha)$, which has normalization similar to that in equation (2). Further, we fix the value of α such that both the form factors have same rms radius. Thus, we have two form factors with same normalization and rms radius but different shapes. To see the effect of such pair of form factors we solve the full scattering equation

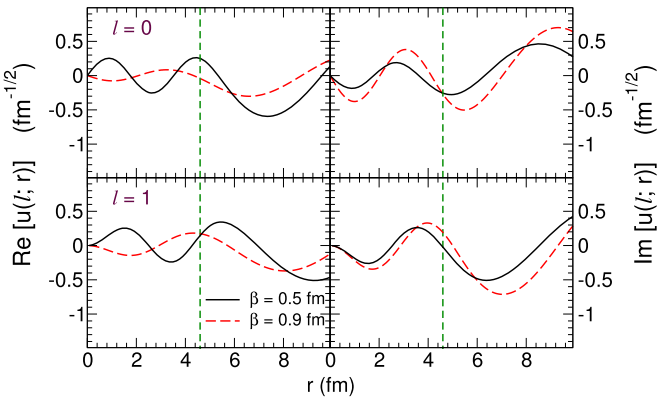

Figure 9. Wave functions corresponding to two values of β as a function of distance. Results are shown for $l = 0$ and 1 for n–^{56}Fe scattering at 10 MeV. Calculations are done with TPM15 parameterization [7]. The vertical dashed line at 4.6 fm marks the radius of ^{56}Fe nucleus.

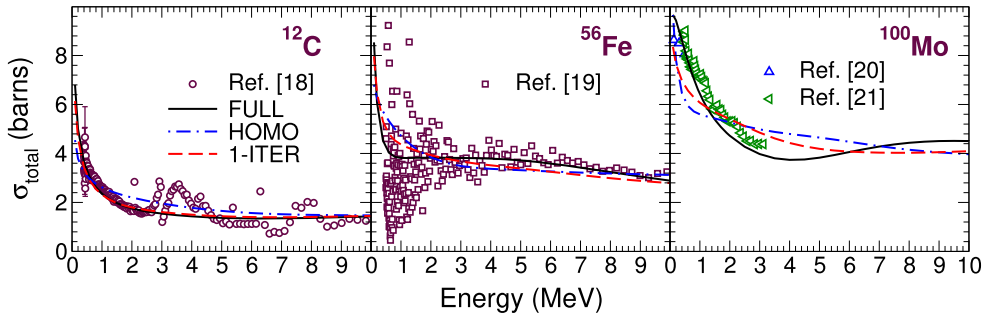

Figure 10. Calculated total cross sections for neutron scattering off ^{12}C, ^{56}Fe and ^{100}Mo nuclei along with the data [18–21]. Calculations are done with TPM15 parameterization [7].

(equation (15)) with these two form factors for $l = 0$ and 1. We find that (i) the two wave functions are very close to each other in magnitude and shape inside the nucleus, and (ii) on the surface both of them have very close logarithmic derivatives, which, as we know, determine the phase shifts. This allows us to conclude that different form factors having same normalization and same rms radius should give similar results for the scattering as well as the reaction observables on a nucleus.

4.2. Impact of the range of nonlocality

Next we explore the effect of different choices of rms radius for a particular form factor. We take two values of β, i.e., 0.9 and 0.5 fm, for the Gaussian form and plot in figure 9 wave functions for $l = 0$ and 1 for neutron–^{56}Fe scattering at 10 MeV. It is evident that the wave functions change significantly with β in the nuclear interior and beyond. This amount of difference should be seen in nuclear reactions as well.

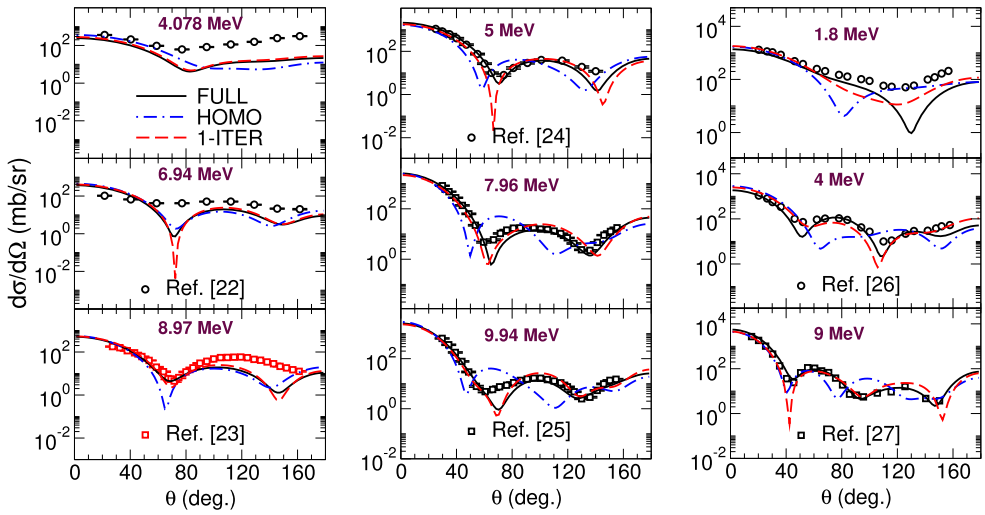

(a) n-^{12}C scattering (b) n-^{56}Fe scattering (c) n-^{100}Mo scattering

Figure 11. Calculated angular distributions using for neutron scattering off ^{12}C, ^{56}Fe and ^{100}Mo nuclei along with the data [22–27]. Calculations are done with TPM15 parameterization [7].

5. Comparison with experiments

Having established the accuracy of our technique, we now present comparison of the calculated observables with the data. However, now in the Schrödinger equation we also include spin-orbit term. The resulting Schrödinger equation is:

$$\left[\frac{\mathrm{d}^2}{\mathrm{d}r^2} - \frac{l(l+1)}{r^2} + \frac{2\mu E}{\hbar^2} + \frac{2\mu V_{\mathrm{SO}}(r)}{\hbar^2} f_{jl}\right] u(j;\, l;\, r) = \frac{2\mu}{\hbar^2}\int_0^{r_m} g(l;\, r,\, r')u(j;\, l;\, r')\mathrm{d}r', \tag{18}$$

$$\begin{aligned} &\text{where } f_{jl} = \frac{1}{2}(j(j+1) - l(l+1) - s(s+1))(\text{with } s = 1/2) \\ &V_{\mathrm{SO}}(r) = (U_{\mathrm{SO}} + \mathrm{i}W_{\mathrm{SO}})s(r) \\ &s(r) = \left(\frac{\hbar^2}{m_\pi{}^2c^2}\right)\left(\frac{1}{a_{\mathrm{so}}r}\right)\exp\left(\frac{r - R_{\mathrm{so}}}{a_{\mathrm{so}}}\right)\left[1 + \exp\left(\frac{x - R_{\mathrm{so}}}{a_{\mathrm{so}}}\right)\right]^{-2}. \end{aligned} \tag{19}$$

For calculating $V_{\mathrm{SO}}(r)$, TPM15 parameterization [7] is used.

As a representation of light and heavy nuclei, we take ^{12}C, ^{56}Fe and ^{100}Mo nuclei and study neutron scattering in the low energy domain up to 10 MeV. In figure 10 we plot the calculated total cross sections for all the three systems along with the experimental data [18–21]. These results are obtained using TPM15 parameterization. Each figure has three curves: HOMO (equation (13)), FULL (equation (15)) and 1-ITER. The 1-ITER results are shown because, as found earlier in section 3, one iteration of equation (15) gives results very close to the full iteration results. Within the spread in experimental numbers, all the calculated results are consistent with the data. In figure 11 we show the various experimental and corresponding calculated angular distributions. We observe that for ^{12}C all the three curves

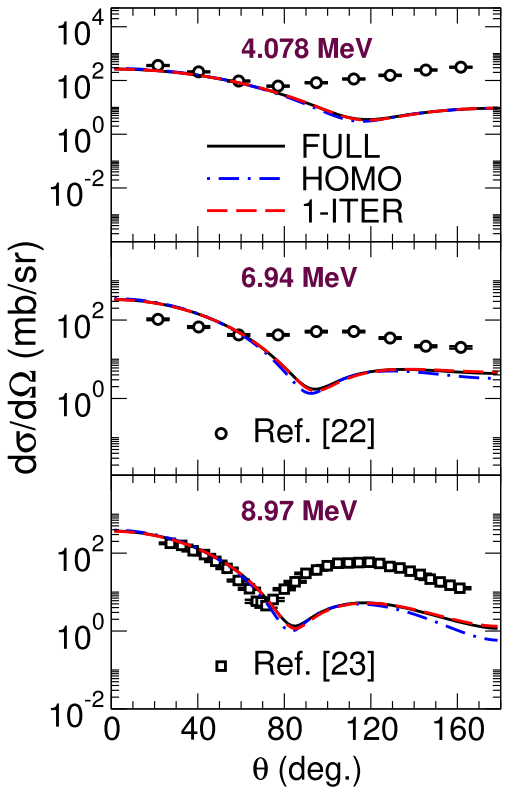

Figure 12. Calculated angular distributions for neutron scattering off ^{12}C nucleus along with the data [22, 23]. Calculations are done using FoldTPM15 prescription.

are reasonably consistent with the data. For heavier nuclei, ^{56}Fe and ^{100}Mo, while 1-ITER and FULL results are in good accord with the data, the HOMO results fall short of it.

For ^{12}C it may be mentioned that, as the TPM15 parameters are obtained by fitting nucleon scattering data on ^{27}Al to ^{208}Pb nuclei, probably a better agreement might be achieved if more appropriate choice of potential is made. To test this possibility, in figure 12 we show the calculated angular distribution using FoldTPM15 prescription for n–^{12}C scattering. These results reproduce the data well only in the forward hemisphere in magnitude and shape. This indicates that there is room for improvisation in the mean field sector for such systems. It may however be mentioned here, as stated earlier in the paper, this improved agreement may be due to reduced nonlocality displayed in FoldTPM15.

6. Summary and conclusion

A novel technique to solve the integro-differential equation in scattering studies has been developed. It is achieved by applying the MVT of integral calculus and using the symmetry of the kernel in the nonhomogeneous term about $r = r'$. The extent of accuracy of the method is established by comparing the solution of the homogeneous equation (equation (13)) thus obtained, with that of the full nonhomogeneous equation (equation (15)). The later is obtained using the iterative scheme initiated by solution of the homogeneous equation. It is found that,

though the solution of the homogeneous equation have some variance with full results, in the first iteration itself this difference practically disappears. The method is independent of the choice of the form of the nonlocality. Hence, it can be used to study the sensitivity to the form of the nonlocality in scattering problems. The effective local potential appearing in the resultant homogeneous equation is different in shape and magnitude in nuclear interior as compared to the local part used in the original nonlocal potential. Further, this effective potential is found to be *l*-dependent, but energy independent. The total and differential cross sections calculated in the low beam energy range (up to around 10 MeV) for neutron scattering off ^{12}C, ^{56}Fe and ^{100}Mo nuclei compare to a reasonable extent with the corresponding measured values. However, the 1-ITER results are found to be in good agreement with the data.

Acknowledgments

We thank Swagata Sarkar and R C Cowsik for a number of illuminating discussions. We are thankful to the referee for constructive criticism and several pertinent observations. NJU acknowledges financial support from Science and Engineering Research Board (SERB), Govt. of India (grant number YSS/2015/000900). AB acknowledges financial support from Dept. of Science and Technology, Govt. of India (grant number DST/INT/SWD/VR/P-04/2014).

ORCID iDs

N J Upadhyay https://orcid.org/0000-0003-2465-2479

References

[1] Bethe H A 1956 *Phys. Rev.* **103** 1353
[2] Frahn W E 1956 *Nuovo Cimento* **4** 313
[3] Frahn W E and Lemmer R H 1957 *Nuovo Cimento* **5** 1564
[4] Lemere M, Stubeda D J, Horiuchi H and Tang Y C 1979 *Nucl. Phys.* A **320** 449
[5] Balantekin A B, Beacom J F and Candido Ribeiro M A 1997 *J. Phys. G: Nucl. Part. Phys.* **24** 2087
[6] Perey F and Buck B 1962 *Nucl. Phys.* **32** 253
[7] Tian Y, Pang D-Y and Ma Z-Y 2015 *Int. J. Mod. Phys.* E **24** 1550006
[8] Kim B T and Udagawa T 1990 *Phys. Rev.* C **42** 1147
[9] Kim B T *et al* 1992 *Comput. Phys. Commun.* **71** 150
[10] Ali S, Rahman M and Husain D 1972 *Phys. Rev.* D **6** 1178
[11] Ahmad A A Z, Ali S, Ferdous N and Ahmed M 1975 *Nuovo Cimento* **30** 385
[12] Rawitscher George H 2012 *Nucl. Phys.* A **886** 1 and references cited therein
[13] Rotureau J *et al* 2017 *Phys. Rev.* C **95** 024315
[14] Atkinson K E 2008 *An Introduction to Numerical Analysis* (New York: Wiley)
[15] Satchler G R and Love W G 1979 *Phys. Rep.* **55** 183
[16] Bertsch G F, Borysowicz J, Mcmanus H and Love W G 1977 *Nucl. Phys.* A **284** 399
[17] Gambhir Y K, Ring P and Thimet A 1990 *Ann. Phys.* **198** 132 and references cited therein
[18] Rapp M J *et al* 2012 *Nucl. Sci. Eng.* **172** 268
[19] Geel W 1995 (EXFOR ENTRY Nos. 22314:2, 22315:1, 22316:1, 22319:2, 22332:1, 22333:1)
[20] Divadeenam M, Bilpuch E G and Newson H W 1968 *Diss. Abs.* B **28** 3834
[21] Pasechnik M V *et al* 1980 *5th All-Union Conf. on Neutron Physics* vol 1 *(Kiev)* p 304
[22] White R M, Lane R O, Knox H D and Cox J M 1980 *Nucl. Phys.* A **340** 13

[23] Glasgow D W *et al* 1976 *Nucl. Sci. Eng.* **61** 521
[24] Kinney W E 1968 Neutron elastic and inelastic scattering from 56Fe from 4.60 to 7.55 MeV *Technical Memo* No. 2052 Oak Ridge National Laboratory (EXFOR ENTRY No. 11708:1)
[25] El-Kadi S M *et al* 1982 *Nucl. Phys.* A **390** 509
[26] Smith A B, Guenther P and Whalen J 1975 *Nucl. Phys.* A **244** 213
[27] Rapaport J *et al* 1979 *Nucl. Phys.* A **313** 1